EASR

Engineering and Applied Science Research

https://www.tci-thaijo.org/index.php/easr/index

Published by the Faculty of Engineering, Khon Kaen University, Thailand

Adsorption of cationic dye on activated carbon from hydrolyzed *Dipterocarpus alatus* leaves: Waste from biodiesel production

Warangkana Khangwichian[1)], Sudarat Pattamasewe[1)], Ratanaporn Leesing[2)], Jesper T.N. Knijnenburg[3)] and Yuvarat Ngernyen*[1)]

[1)]Biomass & Bioenergy Research Laboratory, Department of Chemical Engineering, Faculty of Engineering, Khon Kaen University, Thailand
[2)]Department of Microbiology, Faculty of Science, Khon Kaen University, Thailand
[3)]Biodiversity and Environmental Management Division, International College, Khon Kaen University, Khon Kaen, Thailand

Received 28 September 2021
Revised 4 February 2022
Accepted 7 March 2022

Abstract

In this study, hydrolyzed *Dipterocarpus alatus* leaves (HDL), waste from biodiesel production, were used as precursor to prepare activated carbon. The HDL residue was treated with 30 wt% $ZnCl_2$ (raw material:$ZnCl_2$ solution = 1:2 by weight) for 1 to 24 h followed by carbonization at 500 °C for 1 h in N_2 atmosphere. The highest specific surface area of 497 m^2 g^{-1} was obtained with 12 h treatment. The physicochemical properties of the optimum carbon were investigated by thermogravimetric analysis (TGA), Fourier transform infrared (FTIR) spectroscopy, proximate analysis, bulk density and pH, and the potential of the activated carbon for methylene blue (MB) adsorption was tested under various contact times and initial dye concentrations. Adsorption equilibrium was reached within 50 min. The adsorption of MB onto the HDL-derived activated carbon followed pseudo-second order kinetics through chemisorption, with intra-particle diffusion as the significant controlling step. The Langmuir isotherm provided a better fit of the adsorption equilibrium than the Freundlich isotherm, with a maximum monolayer adsorption capacity of 338.86 mg g^{-1}. The activated carbon prepared from *Dipterocarpus alatus* leaves residue exhibited good adsorption uptake for MB and therefore presents an attractive and effective adsorbent for cationic dyes.

Keywords: Activated carbon, *Dipterocarpus alatus* leaves, Chemical activation, Adsorption, Cationic dye

1. Introduction

Due to the growing energy demand, limited availability of fossil fuel resources and environmental concerns, the development of sustainable biomass-based fuels has received great consideration. As a promising alternative, oleaginous microorganisms (yeasts, fungi, microalgae, and bacteria) can accumulate significant quantities of lipids. These single cell oils have fatty acid profiles similar to those of vegetable oils that are traditionally used as feedstock for biodiesel production. However, biofuel production using single cell oils from oleaginous microorganisms is hampered due to the high cost of sugar-based growth substrates. Therefore, inexpensive and abundantly available growth substrates are required. Lignocellulosic biomass can serve as sugar source for the culturing of oleaginous microorganisms because it contains a significant proportion of polysaccharides or polymeric carbohydrates (cellulose and hemicelluloses). The breakdown of these carbohydrates can produce hexose and pentose sugars [1]. Pretreatment of the lignocellulosic biomass is required for degradation, using techniques such as dilute acid hydrolysis [2].

Dipterocarpus alatus is a timber tree found in Thailand, Vietnam, Cambodia, Laos, Myanmar, Philippines and India. Its wood is used for construction and its resin is used for illumination, lighting and waterproofing baskets and boats, used in printing ink industries and making paint, varnish and lacquer [3]. The leaves of *Dipterocarpus alatus* present a valuable sustainable growth substrate for oleaginous microorganisms. However, after acid hydrolysis, a solid leaf residue remains, which should be considered for zero waste approach and value-added product.

Activated carbon is a highly porous material that can be produced by pyrolysis of carbonaceous materials. Due to the high production costs, lignocellulosic materials from agricultural and forestry residues are preferred raw materials due to their low cost and wide availability. Activated carbons can be produced via physical or chemical activation process. Physical activation is performed in two steps, i.e. carbonization and activation, whereas chemical activation is achieved in one step in which the activation and carbonization process are combined. In the chemical activation, the starting material is treated with an activating agent such as $ZnCl_2$, KOH, NaOH, H_3PO_4 or H_2SO_4 and the treated raw material is carbonized at a temperature typically between 400 and 800 °C in an oxygen-free atmosphere. For physical activation, the precursor is carbonized (below 700 °C) followed by activation of the resulting char with an activating agent such as CO_2 or steam at 700-1100 °C [4, 5]. Chemical activation is generally preferred over physical activation due to the one-step simple process and lower activation temperature resulting in higher activated carbon yield and better development of porous structure [6, 7]. However, the resulting activated carbons from chemical activation require a washing step to remove any residual activating agent.

*Corresponding author.
Email address: nyuvarat@kku.ac.th
doi: 10.14456/easr.2022.52

The leaves from various plants have been utilized for the preparation of activated carbons. For example, Rashid et al. used coconut leaves for the production of carbon using $FeCl_3$ activation [8]. Anisuzzaman et al. prepared carbon from *Typha orientalis* or cattail leaves via activation with H_3PO_4 [9]. Banana leaves were used as starting material for the preparation of six different carbons by chemical activation with H_3PO_4 [10]. Patil et al. explored the feasibility of sugar cane leaves as an alternative precursor for preparation of carbon using $ZnCl_2$ activation [11]. Other studies used palm tree leaves activated by $ZnCl_2$ [12] and reedy grass leaves by H_3PO_4 [13].

Methylene blue (MB) is a cationic basic dye primarily used in textile, paper, leather, plastic, and automotive industries. About 10-15% of used dye is lost in the effluent of the dyeing process, which can cause allergic dermatitis, skin irritation, vomiting, eye burns, shock, cyanosis, jaundice, quadriplegia, cancer and mutations [7, 14, 15]. Therefore, the treatment of effluents containing dyes is a priority. Various techniques have been used to remove color of dyes from wastewater including oxidation, coagulation and flocculation, photodegradation, solvent extraction, ultrafiltration, reverse osmosis, biodegradation and adsorption [7, 14, 16]. Adsorption is generally preferred because of its simple design, ease of operation, low cost and high efficiency with low adsorbent dosage and process time [17, 18]. Various adsorbents have been used to remove dyes from solution such as multiwalled carbon nanotubes [16], metal-organic framework nanocomposites [19], carbon nanotube/metal-organic framework nanocomposites [18] or magnetic ferrite nanoparticles [20]. In addition to these materials, activated carbon is also an efficient adsorbent to remove dyes from wastewater due to the high surface area and adsorption capacity. Many researchers have used activated carbon from biomass wastes to adsorb MB from solution, such as peach stones [21], cotton stalk [22], hulls [23], jute fiber [24], oil palm shell [25], date stone [26], piassava fibers [27], jackfruit peel [28], walnut shell [29], black stone cherries [30] or waste cotton fibers [31]. To the best of our knowledge, activated carbon prepared from *Dipterocarpus alatus* leaves have not been used as starting material to study MB adsorption.

The objective of the present study was to prepare activated carbon from *Dipterocarpus alatus* leaves residue from acid hydrolysis process (HDL) and to optimize the activation conditions. From our previous studied [32], using different chemical activating agents (H_3PO_4, HNO_3, KOH, NaOH, $ZnCl_2$ and $FeCl_3$) demonstrated that activation of HDL with $ZnCl_2$ for 1 h produced an activated carbon with the highest surface area. Therefore, $ZnCl_2$ was selected as activating agent and the conditions were further optimized. The HDL was chemically activated with $ZnCl_2$ for 1 to 24 hours and subsequently carbonized at 500 °C for 1 h. The prepared carbons were analyzed by TGA, proximate analysis, nitrogen gas adsorption, FTIR spectroscopy, bulk density and pH. Adsorption properties of the obtained carbons were investigated for their ability to remove MB from aqueous solution under varying adsorption times and initial dye concentrations. Adsorption kinetics and isotherms were studied and modeled with well-known mathematical equations.

2. Experimental

2.1 Materials

The hydrolyzed *Dipterocarpus alatus* leaves (HDL) in powder form were collected from the Department of Microbiology, Faculty of Science, Khon Kaen University. The HDL samples were sieved with mesh no. 18 to obtain a fine powder (< 1 mm). Methylene blue (MB) was supplied by Ajax Finechem (82% purity). A stock MB solution of 1000 mg L^{-1} was prepared and the required concentrations for the adsorption study were obtained by dilution in DI water. Other chemicals were analytical grade and used without further purification.

2.2 Preparation of activated carbon

For chemical activation, 5 g of HDL was treated with 10 g of a 30% w/w $ZnCl_2$ solution to obtain a weight ratio of 1:2 (HDL:$ZnCl_2$ solution). This weight ratio was selected because of the low density of HDL. A lower weight ratio (less than 2 times) resulted in incomplete wetting of HDL with the $ZnCl_2$ solution, whereas a higher ratio will result in higher cost. The treatment time was varied from 1 to 24 h and was carried out at room temperature without any mechanical stirrer. Under these conditions, the complete $ZnCl_2$ solution penetrated into the HDL and there was no excess solution. The activated HDL was collected with a stainless steel laboratory spoon and subsequently carbonized in a high temperature furnace at 500 °C for 1 h under continuous N_2 flow (200 mL min^{-1}) with a heating rate of 30 °C min^{-1}. The resulting activated carbon was washed with DI water until the pH of the washing effluent was equal to the starting water, in order to remove the remaining $ZnCl_2$ and possible impurities that were generated during carbonization. Finally, the sample was dried in an oven (Memmert UNE 500) at 105 °C for 3 h.

The production yield of the activated carbon was determined through equation (1)

$$\text{Yield (wt\%)} = \frac{W_{ac}}{W_i} \times 100 \quad (1)$$

where W_{ac} and W_i are the weight of carbon and the initial mass of HDL, respectively.

2.3 Characterization

Proximate analysis of HDL and obtained activated carbons including moisture, ash, volatile matter and fixed carbon contents was performed according to standard methods. The moisture content was determined following ASTM D2867 method using oven (Memmert UNE 500) drying. The sample was placed into a pre-weighed ceramic crucible and dried at 150 °C for 3 h. The sample was weighed after cooling down and the moisture content was calculated by equation (2):

$$\text{Moisture (wt\%)} = \frac{W_1 - W_2}{W_1} \times 100 \quad (2)$$

where W_1 is the weight of the original (wet) sample and W_2 is the weight of the dried sample. The dried sample was heated at 950 °C for 30 min in a muffle furnace (VULCAN TM3-550) according to ASTM D5832-98 method, and the volatile matter was calculated using equation (3):

$$\text{Volatile matter (wt\%)} = \frac{W_2 - W_3}{W_2} \times 100 \quad (3)$$

where W_3 is the weight after heating. The residual sample was ashed at 800 °C for 2 h in a muffle furnace and the ash content was calculated as follows:

$$\text{Ash (wt\%)} = \frac{W_4}{W_2} \times 100 \quad (4)$$

where W_4 is the ash weight. All measurements were determined in triplicate and the average values are reported. Finally, the fixed carbon content was calculated by 100% - volatile matter (%) - ash (%).

The thermal behavior (TG-DTA curves) of the raw material and activated carbons was studied with a Thermogravimetric Analyzer (DTG 60H, Shimadzu). About 10 mg of each sample was loaded into a platinum pan and heated from room temperature to 950 °C with a heating rate of 10 °C min^{-1} under N_2 flow of 60 mL min^{-1}.

Porous properties of the activated carbon were studied by N_2 adsorption at 77 K using a Surface Area and Porosimetry Analyzer (ASAP 2460, Micromeritics). Prior to the analysis, the sample was outgassed at 150 °C until the pressure was less than 100 mTorr. The specific surface area, S_{BET}, of the carbon was calculated using the Brunauer-Emmett-Teller (BET) equation. The micropore volume, V_{mic}, was determined from the t-plot and the total pore volume, V_T, was estimated as the nitrogen gas adsorbed at P/P^o of about 0.99. The mesopore volume, V_{meso}, was determined by the difference between V_T and V_{mic}. The average pore size, D_P, was determined by the Barrett-Joyner-Halenda (BJH) method using desorption data.

The surface functional groups of the activated carbon were studied by Fourier Transform infrared spectroscopy (FTIR) using a Bruker ALPHA II. The activated carbon was dispersed into potassium bromide (KBr) tablets and spectra were recorded from 4000 to 550 cm^{-1}.

The bulk density (i.e., the mass of a unit volume including both pore system and voids between particles) of the activated carbons was determined following Ahmedna et al. [33]. A 10 cm^3 glass cylinder was filled with activated carbon and the bulk density (g/cm^3) was calculated using equation (5):

$$\text{Bulk density} = \frac{W_{ac}}{V_c} \quad (5)$$

where W_{ac} (g) is the weight of carbon and V_c (cm^3) is cylinder volume.

The pH of activated carbon in distilled water was measured following Ekpete et al. [34]. Here, 100 mL of distilled water containing 1 g of carbon was boiled for 5 minutes. The pH was measured by using a pH meter (Ohaus ST3100-F) after addition of 100 mL of distilled water (total volume of solution 200 mL) and cooling to room temperature.

2.4 Methylene blue adsorption studies

Adsorption studies were performed in batch mode at room temperature. The adsorption kinetics were determined by adding 0.05 g activated carbon to 50 mL of MB solution with an initial concentration of 6 mg L^{-1} for different times varying from 5 to 180 min. After the desired contact time was reached, the activated carbon was separated from the dye solution by filtration. The residual MB concentration in the filtrate was analyzed by UV-vis spectrophotometer (Agilent 8453) at the peak wavelength of 668 nm. The adsorbed amount of MB at time t, q_t (mg g^{-1}), was calculated by

$$q_t = \frac{(C_o - C_t)V}{W} \quad (6)$$

where C_o and C_t (mg L^{-1}) are the MB concentrations at initial and time t, respectively, V (L) is the volume of dye solution and W (g) is the weight of activated carbon used.

The adsorption isotherm was measured by adding 0.05 g of carbon into 50 mL MB solution with different initial concentrations from 30 to 600 mg L^{-1} without pH adjustment and kept for 50 min (this equilibrium time was determined in the previous experiment). The equilibrium MB concentrations were measured by UV-vis spectrophotometer and the equilibrium adsorption capacity, q_e (mg g^{-1}), was calculated by

$$q_e = \frac{(C_o - C_e)V}{W} \quad (7)$$

where C_e (mg L^{-1}) is the concentration of MB at equilibrium.

3. Results and discussion

3.1 Properties of raw material

The proximate analysis results of hydrolyzed *Dipterocarpus alatus* leaves (HDL) are shown in Table 1. The moisture content of 12.61 wt% in the HDL can be ascribed to water. The HDL shows a high volatile matter content (78.51 wt%) and average contents of ash (12.22 wt%) and fixed carbon (9.27 wt%). The high volatile matter makes HDL a good starting material for preparation of activated carbon [35]. Ash is a non-carbon or mineral substance that typically comprises 1-20% depending on the raw material [36].

Figure 1 shows the TG and DTA curves of hydrolyzed *Dipterocarpus alatus* leaves (HDL). The weight loss from the TG curve can be divided into three stages. The first stage occurs with a weight loss of 15% between 30 and 110 °C that is attributed to adsorbed water. The corresponding endothermic DTA peak at around 70 °C was also found for *Casuarina equisetifolia* fruit waste [37]. The

second stage with a weight loss of 68% takes place at around 200 to 450 °C, which is attributed to the thermal degradation of hemicellulose and cellulose accompanied by the formation of tar and gases such as CO and CO_2 [38, 39]. In this stage, two exothermic DTA peaks are observed at around 330 and 390 °C. Similar results have been reported in literature for pyrolysis of other biomass materials such as walnut shell [39]. The third weight loss stage takes place from 450 to 950 °C, with a smaller weight loss than the second stage. This stage could be due to lignin decomposition that results in a carbonaceous residue [38, 39]. The shoulder DTA peak at 460 °C is similar to that observed in activated carbon production from *Casuarina equisetifolia* fruit waste [37]. The final residue that remains is approximately 15% of the initial weight. The results of the thermal analysis indicate that the optimum carbonization temperature for the HDL is at 500 °C or higher, where no significant weight loss takes place. Therefore, in this research 500 °C was chosen as the carbonization temperature.

Table 1 Physicochemical of raw material (HDL) [32] and optimum activated carbon prepared from HDL after 12 h treated with $ZnCl_2$.

Property	Value
Hydrolyzed *Dipterocarpus alatus* leaves (HDL)	
Moisture (wt%, wet basis)	12.61
Ash (wt%, dry basis)	12.22
Volatile matter (wt%, dry basis)	78.51
Fixed carbon (wt%, dry basis)	9.27
Optimum activated carbon	
Moisture (wt%, wet basis)	13.42
Ash (wt%, dry basis)	9.44
Volatile matter (wt%, dry basis)	14.19
Fixed carbon (wt%, dry basis)	76.37
Bulk density (g cm^{-3})	0.44
pH	6.99

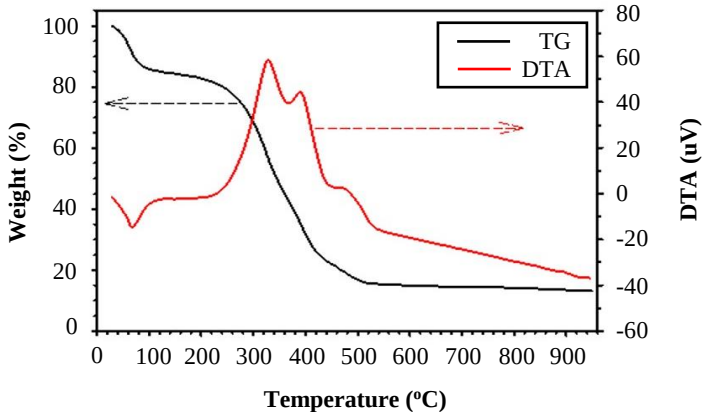

Figure 1 Thermal analysis data (TG and DTA) in N_2 atmosphere of hydrolyzed *Dipterocarpus alatus* leaves (HDL).

3.2 Porous structure and yield of the activated carbon

Figure 2 shows the N_2 isotherms of prepared carbons for different activation times. The adsorption-desorption isotherm for 1 h activation has been presented in our previous work [32]. The isotherms of all activation times show a similar trend with an upward shift with increasing activation time from 1 to 12 h, and then the amount adsorbed decreases for 24 h. All isotherms are classified as IUPAC Type IV that are indicative of mesoporous materials. The slope of the adsorption isotherms gradually increases and exhibits a hysteresis loop at around P/P^o = 0.4-1, indicating capillary condensation in the mesopores. Similar findings indicating the presence of both micropores and mesopores were also reported elsewhere. For example, Angın et al. [40], Mahamad et al. [41] and Yagmur et al. [42] used $ZnCl_2$ to activate safflower seed press cake, pineapple waste and oleaster fruit, respectively.

The effect of activation time on the yield and porous properties of the obtained activated carbons is presented in Table 2. The BET surface area increased with an increase in activation time from 1 to 12 h. The data for 1 h activation from our previous work [32] are also shown here for comparison. The activation process improves the pore development and creates new pores, resulting in an increased surface area for longer activation times. However, further increasing the activation time to 24 h resulted in a slight decrease in surface area. The long activation time likely resulted in a collapse of some of the pore walls which resulted pore widening [43]. This is also evident from the decrease in V_{mic} and increase in V_{meso}. Gupta and Garg [44] proposed that the chemical activation with $ZnCl_2$, a dehydrating agent, improves the porosity by promoting the aromatization of the carbon skeleton while suppressing tar formation. The maximum S_{BET} of 497 m^2 g^{-1} was obtained after 12 h activation. Therefore, 12 h was selected as the optimum activation time for production of the carbon from HDL.

The total pore volume (V_T) and average pore diameter (D_p) of the prepared carbons increased with activation time. This indicates that increasing the activation time not only created more pores but also increased the pore size of the obtained activated carbons. Adsorbent pores can be classified into (1) micropores with pore diameter less than 2 nm, (2) mesopores with pore diameter between 2-50 nm and (3) macropores with pore diameter larger than 50 nm. When the pore volume is considered, the micropore fraction of all prepared activated carbons (69-79%) is higher than the mesopore fraction (21-31%). The mesoporosity is very important in facilitating the access of the adsorbate molecules to the interior of the activated carbon particles [35]. The average pore size of the carbons is 2.52-2.70 nm. The adsorbate molecules can only penetrate into the adsorbent when the pores have a diameter larger than the molecular diameter of the adsorbate [45]. Methylene blue (MB) has a molecular diameter of 1.382 nm [46]; therefore, all prepared activated carbons are suitable for MB adsorption.

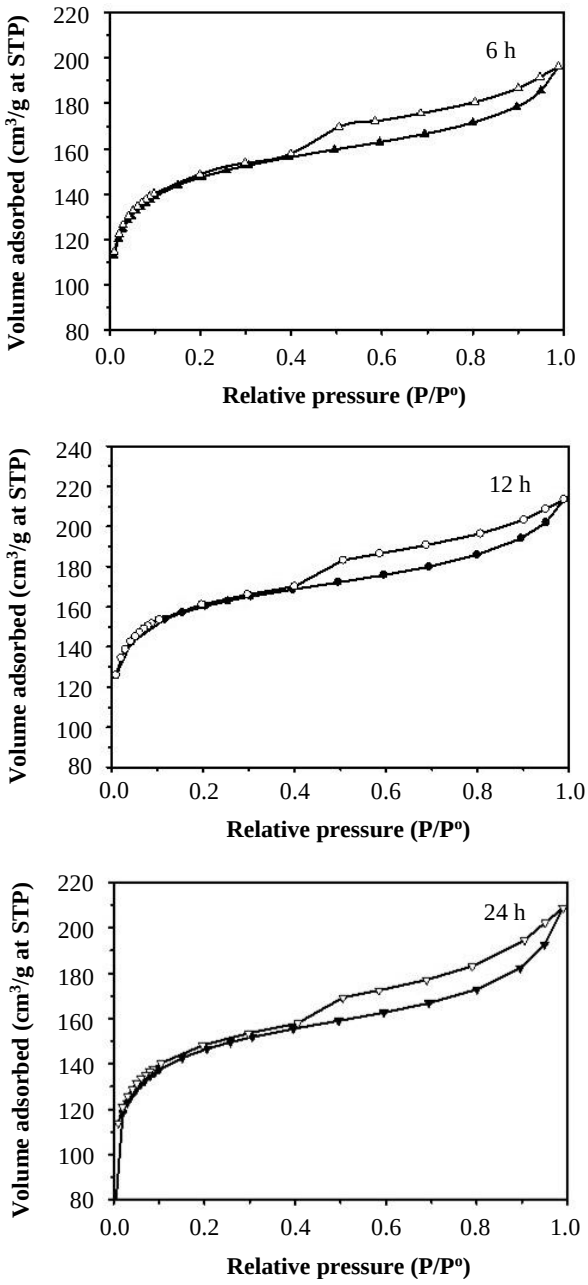

Figure 2 Nitrogen adsorption-desorption isotherms at 77 K for HDL-based activated carbons after different activation times.

Table 2 also shows the yield of activated carbons obtained with varying activation times. The yield slightly decreased from 66 to 60 wt% with increased activation time from 1 to 24 h. In the production of activated carbon, a relatively high yield of carbon is required. The range of yields obtained (60-66 wt%) was similar to that reported in other works [39, 47, 48].

Table 2 Yield and porous characteristics of the prepared activated carbons after different activation times.

Activation time (h)	Yield (wt%)	S_{BET} ($m^2\ g^{-1}$)	V_{mic} ($cm^3\ g^{-1}$)	V_{meso} ($cm^3\ g^{-1}$)	V_T ($cm^3\ g^{-1}$)	D_p (nm)
1	66	456	0.22 (73%)	0.08 (27%)	0.30	2.52
6	62	481	0.22 (73%)	0.08 (27%)	0.30	2.63
12	60	497	0.26 (79%)	0.07 (21%)	0.33	2.65
24	60	479	0.22 (69%)	0.10 (31%)	0.32	2.70

Table 3 indicates the potential of hydrolyzed *Dipterocarpus alatus* leaves (HDL) for the preparation of carbon. The surface area and total pore volume of the optimum carbon was similar to or higher than activated carbons prepared from other biomasses. The HDL-derived activated carbon also had surface area similar to commercial activated carbons such as CAC (515 $m^2\ g^{-1}$) [44]. Pastor-Villegas et al. [49] reported that all industrial adsorbents have large specific surface areas generally well in excess of 100 $m^2\ g^{-1}$ and the total pore volume of activated carbon usually exceeds 0.2 $cm^3\ g^{-1}$. Therefore, HDL, a solid waste from biodiesel production, is an attractive raw material for production of activated carbon. To avoid Zn leaching during use, Rozada et al. [50] suggested two possible treatments: one consisting of a coating with a polymer and another involving successive washing stages.

Table 3 Comparison of porous properties of the prepared HDL-derived carbon with previous studies.

Raw material	Preparation conditions	Porous properties
Hydrolyzed *Dipterocarpus alatus* leaves (HDL)	Soaking: $ZnCl_2$ 30 wt%, chemical ratio 1:2, 12 h Carbonization: 500 °C, 1 h	S_{BET} = 497 $m^2 g^{-1}$ V_T = 0.33 $cm^3 g^{-1}$
Peanut shell [51]	Soaking: KOH 20%, impregnation ratio 1:1, 24 h, room temperature Carbonization: 170 °C for 1 h, then 450 °C for 1 h under N_2 or 450°C for 1 h under air	S_{BET} = 88.85-95.51 $m^2 g^{-1}$ V_T = 0.33-0.35 $cm^3 g^{-1}$
Palm kernel shell [52]	Carbonization: 400 °C, 1 h Soaking: KOH, impregnation ratio 1:1, 80 °C, 2 h Activation: 800-1,000 °C, 15-45 min	S_{BET} = 17-217 $m^2 g^{-1}$ V_T = 0.015-0.12 $cm^3 g^{-1}$
Jowar Stalk [15]	Soaking: H_2SO_4 50 (v/v), 24 h Carbonization: 800 °C, 0.5 h	S_{BET} = 292 $m^2 g^{-1}$ V_T = 0.31 $cm^3 g^{-1}$
Kenaf core fiber [53]	Carbonization: 400 °C, 1 h Soaking: H_3PO_4 30 %, impregnation ratio 1:4 Activation: 500 °C, 1 h	S_{BET} = 299 $m^2 g^{-1}$
Palm tree leaves [12]	Soaking: $ZnCl_2$, impregnation ratio 1:1.5, 24 h Carbonization: 500 °C	S_{BET} = 299.84 $m^2 g^{-1}$ V_T = 0.129 $cm^3 g^{-1}$
Black gram husk and millet husk [54]	Soaking and carbonization: H_3PO_4 450 °C, 1 h	Millet husk: S_{BET} = 397 $m^2 g^{-1}$, V_T = 0.67 $cm^3 g^{-1}$ Black gram husk: S_{BET} = 480 $m^2 g^{-1}$, V_T = 0.50 $cm^3 g^{-1}$
Macadamia nutshell [55]	Carbonization: 350 °C, 1 h Soaking: H_2SO_4 50% or K_2CO_3, impregnation ratio 1:1, 24 h Calcination: 650 °C	H_2SO_4: S_{BET} = 426 $m^2 g^{-1}$, V_T = 0.21 $cm^3 g^{-1}$ K_2CO_3: S_{BET} = 460 $m^2 g^{-1}$, V_T = 0.23 $cm^3 g^{-1}$
Casuarina equisetifolia fruit waste [37]	Carbonization: 300 °C, 1 h Soaking: $ZnCl_2$ or KOH or H_3PO_4 10 %, impregnation ratio 4:1, overnight Activation: 700 °C, 1 h	$ZnCl_2$: S_{BET} = 335 $m^2 g^{-1}$, V_T = 0.42 $cm^3 g^{-1}$ KOH: S_{BET} = 514 $m^2 g^{-1}$, V_T = 0.45 $cm^3 g^{-1}$ H_3PO_4: S_{BET} = 548 $m^2 g^{-1}$, V_T = 0.43 $cm^3 g^{-1}$
Pomegranate seeds [56]	Soaking: $ZnCl_2$, 24 h Carbonization: 600 and 800 °C, 1 h	S_{BET} = 455.3-978.8 $m^2 g^{-1}$ V_T = 0.217-0.563 $cm^3 g^{-1}$

3.3 Characterization of the optimum activated carbon

As described in the previous section, the optimum activation time that gave the highest surface area of carbon (497 $m^2 g^{-1}$) was 12 h. Therefore, this activated carbon was characterized in detail and used as adsorbent for MB adsorption. Thermal analysis of the optimum activated carbon is presented in Figure 3. The activated carbon did not show a significant weight loss until the temperature exceeded 400 °C, where a weight loss of 28% was observed. According to the TG curves presented in Figure 3b, the thermal decomposition of the activated carbon was significantly different from the raw material (hydrolyzed leaves). The activated carbon shows a higher thermal stability with total weight loss of 45% compared to 87% for HDL. This was due to the fact that during the carbonization process, tar and volatile compounds were removed. The DTA curve of activated carbon shows that thermal degradation occurred at around 80 and > 420 °C, which may be due to dehydration and destruction of organic matter [57]. The shape of the TG curve of the prepared carbon is similar to previous studies [6, 58-60].

Table 1 also shows the results of proximate analysis and bulk density of the optimum activated carbon. Compared to the HDL, the fixed carbon increased from 9.27 to 76.37 wt% whereas the volatile matter decreased from 78.51 to 14.19 wt%. This is because the volatile matter was released during carbonization as liquid and gas, leaving a material with high purity carbon. The increase in fixed carbon and moisture contents and decrease in volatile matter content of activated carbon compared to the HDL are in agreement with previous studies [61]. The ash content of the activated carbon slightly decreased compared to the starting material. This can be attributed to the washing step with DI water that likely removed water-soluble minerals from the activated carbon. A high ash content reduces the mechanical strength of a carbon which negatively affects the adsorption capacity [34, 47]. Abdullah et al. [47] also suggest that the ash content of activated carbons used as adsorbent should be within a range of 1-20%. The HDL-derived activated carbon in the current study falls within this range.

The bulk density of material depends on the shape, size and density of the individual particles [36]. The bulk density of the optimum carbon was 0.44 g cm^{-3}, which is comparable to previous studies. For example, Ravichandran et al. [37] found that KOH, $ZnCl_2$ and H_3PO_4 activation of *Casuarina equisetifolia* fruit waste resulted in a bulk density of 0.40, 0.43 and 0.49 g cm^{-3}, respectively, and the bulk density of activated carbons prepared from plantain (*Musa paradisiaca*) fruit stem with H_3PO_4 and $ZnCl_2$ activation were 0.32 and 0.34 g cm^{-3} [34], respectively. The bulk density for activated carbons used in gas adsorption range from 0.40 to 0.50 g cm^{-3}, while those used in decolorization have a bulk density ranging from 0.25 to 0.75 g cm^{-3} [49]. Therefore, the optimum HDL-derived activated carbon will be suitable for color removal purpose. Ademiluyi and David-West [62] also proposed that a low bulk density of activated carbon stimulates quick adsorption in gas and liquid phase systems.

The pH of the activated carbon directly influences the adsorption process and a neutral pH (6-8) is generally preferred [37]. Table 1 shows that $ZnCl_2$ activation gave activated carbon with a pH of 6.99. In contrast, Ekpete et al. [34] and Ravichandran et al. [37] reported that the pH values of carbons prepared from $ZnCl_2$ activation of plantain fruit stem and *Casuarina equisetifolia* fruit waste were 9.30 and 9.78, respectively. A different pH value may be due to differences in raw material, preparation process and even washing method [37].

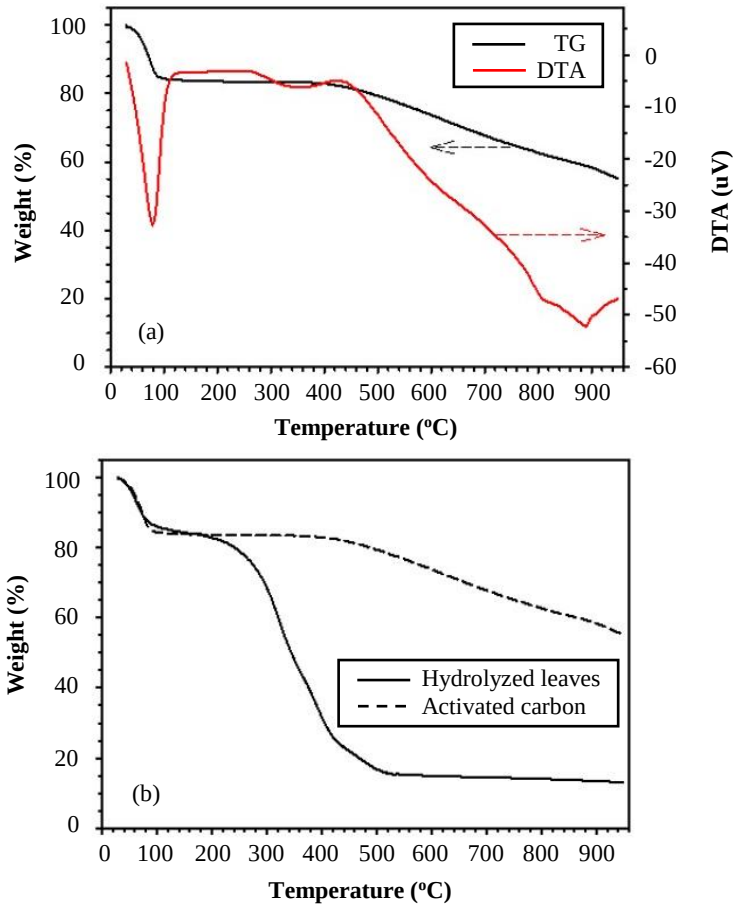

Figure 3 (a) TG and DTA curves of the optimum activated carbon prepared after 12 h treated with $ZnCl_2$ and (b) TG curve of activated carbon compare with raw material (hydrolyzed leaves).

A qualitative investigation of the surface functional groups was carried out by FTIR as shown in Figure 4. The broad band at 3384 cm^{-1} of hydrolyzed leaves corresponds to -OH vibrations that probably originate from hydroxyl groups, while a strong broad band at 3418 cm^{-1} of activated carbon corresponded to -OH group from an alcohol [34]. The presence of this group in the raw material and activated carbon was reported in the literature [34, 52]. The spectra show that some surface groups were removed from the raw material after carbonization, for example at 2114 cm^{-1}, which indicates that a chemical transformation took place during carbonization. The band at 1601 or 1607 cm^{-1} could be ascribed to the stretching vibration of aromatic C=C bonds [63]. The peaks detected around 1000 cm^{-1} could be related to vibrations of C-O functional groups [44] and the peaks around 920 cm^{-1} are assigned to C-H and C-O [32]. The band at around 600 cm^{-1} observed for both samples is associated with out-of-plane angular deformations of benzene derivatives [5]. Verma and Samanta [64] reviewed that the active functional groups that participate in the binding of MB molecules are -OH, C-O, C=O and -COO-. The presence of these functional groups on the HDL-derived activated carbon can help to adsorbed MB, in addition to the specific surface area.

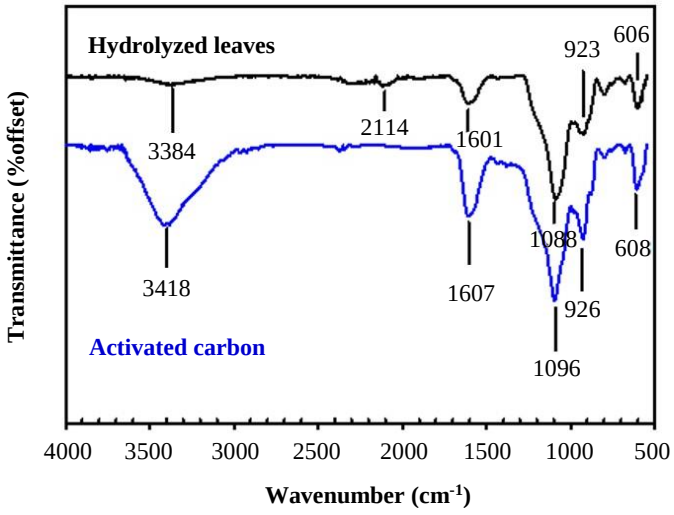

Figure 4 FTIR Spectra of optimum activated carbon compare with the raw material (hydrolyzed leaves).

3.4 Methylene blue adsorption of optimum activated carbon

3.4.1 Adsorption kinetics

The kinetic and equilibrium studies were used to study the adsorption of methylene blue (MB) onto HDL-derived carbon. The effect of contact time on the MB removal at an initial concentration of 6 mg L^{-1} is displayed in Figure 5. The MB adsorbed amount increased with time. The adsorption process is rapid during the first 40 min and equilibrium was reached after 50 min. At the equilibrium point, the MB molecules that are desorbed from the porous materials are in dynamic equilibrium with the MB being adsorbed onto the material. This equilibrium time is used to evaluate the affinity of an adsorbate to porous material [65]. Therefore, the equilibrium time for MB adsorption of the optimum carbon was 50 min, which was chosen for measurement of the adsorption isotherm.

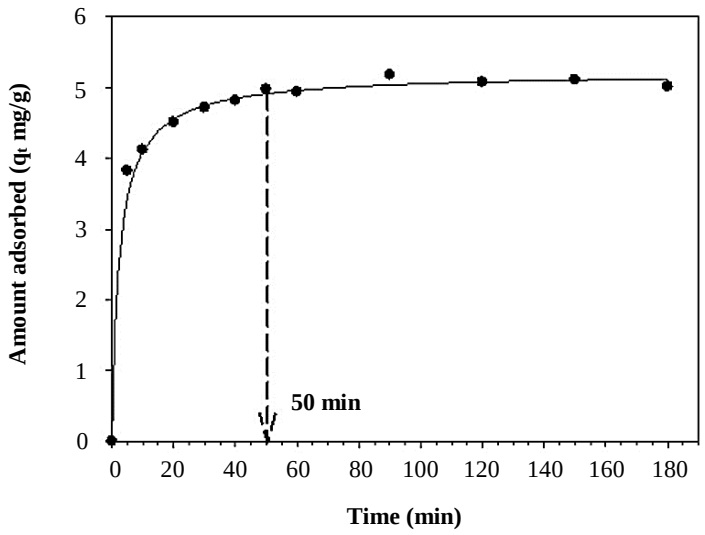

Figure 5 Effect of contact time on the MB adsorption onto optimum carbon.

Methylene blue adsorption onto activated carbon may involve 4 steps including (1) film or external diffusion, (2) pore diffusion, (3) surface diffusion and (4) adsorption on the pore surface [66]. In this study, three kinetic models (i.e., pseudo-first order, pseudo-second order and intra-particle diffusion models) have been applied to the experimental data. The pseudo-first order rate equation is given as [67]:

$$log(q_e - q_t) = logq_e - \frac{k_1 t}{2.303} \quad (8)$$

where q_e and q_t (mg g^{-1}) are the amount of MB adsorbed on activated carbon at equilibrium and time t and k_1 (min^{-1}) is the rate constant. A plot of log(q_e - q_t) versus t from experimental data gives a linear relationship and the value of k_1 can be determined from the slope. The intercept is used to calculate $q_{e,cal}$.

The linearized form of pseudo-second order kinetic model is [67]:

$$\frac{t}{q_t} = \frac{1}{k_2 q_e^2} + \frac{t}{q_e} \quad (9)$$

where k_2 (g mg^{-1} min^{-1}) is the rate constant. A plot of t/q_t versus t from the experimental data gives a linear relationship and $q_{e,cal}$ and k_2 can be calculated from the slope and intercept, respectively.

Figure 6 demonstrates the linear plots of the pseudo-first order and pseudo-second order models, and the obtained parameters along with correlation coefficient or R^2 are summarized in Table 4. The pseudo-first order kinetic is not appropriate to describe the adsorption behavior due to the low R^2 value of 0.771. The calculated amount adsorbed ($q_{e,cal}$) in the pseudo-first order model was also much smaller than the experimentally obtained value ($q_{e,exp}$). This is attributed to the existence of an external boundary layer or mass transfer resistance at the beginning of adsorption, since this model is only suitable for the initial stage of the adsorption process [65]. On the contrary, the pseudo-second order model fits the data very well with a high R^2 value of 0.999, and the q_e value calculated by this model (5.139 mg g^{-1}) is very close to the experimental result (5.181 mg g^{-1}). The pseudo-second order model describes the chemical adsorption of MB onto carbon involving valence forces or electron exchange between adsorbate and adsorbent [68, 69]. Similar findings that MB adsorption onto activated carbon follows pseudo-second order kinetics rather than pseudo-first order have been reported by Geçgel et al. [14], Hameed et al. [70], Ahmad et al. [71] and Ozer et al. [72]. The rate constant k_2 can be used to calculate initial sorption rate as $h = k_2 q_e^2$. The higher value of h indicated a higher initial rate of adsorption. In this case, the h value was equal to 2.535 mg g^{-1} min^{-1}.

The pseudo-first order and pseudo-second order kinetic models do not explain the diffusion mechanism. Hence, the effect of intra-particle diffusion resistance on adsorption can be determined by [67]:

$$q_t = k_a t^{1/2} + C \quad (10)$$

where k_d (mg g^{-1} min$^{-1/2}$) is the constant of this model and constant C (mg g^{-1}) is an approximation of the boundary layer thickness [5]. The values of k_d and C can be obtained from the slope and intercept of the linear plots of q_t versus $t^{1/2}$. As shown in Figure 6 (c) and Table 4, the intra-particle diffusion model also well described the adsorption kinetics (R^2 = 0.999 and 0.990 for the first and second stage, respectively). Figure 6 (c) shows that the diffusion mechanism exhibited two stages and the lines do not cross the origin, indicating that the adsorption is not only rate controlled but also boundary layer diffusion controlled [73]. The first stage is related to transfer of the adsorbate molecules to the external surface of the adsorbent or film diffusion mechanism [5, 44]. The second stage is more gradual and could be attributed to the penetration of adsorbate molecules into inner layers of the adsorbent or intra-particle diffusion mechanism [5, 44]. A similar two stage adsorption process was mentioned for the MB adsorption onto activated carbons derived from other raw materials such as cocoa shell [71], sewage sludge [44], *Lupinus albus* seed [73] and chitosan flakes [66].

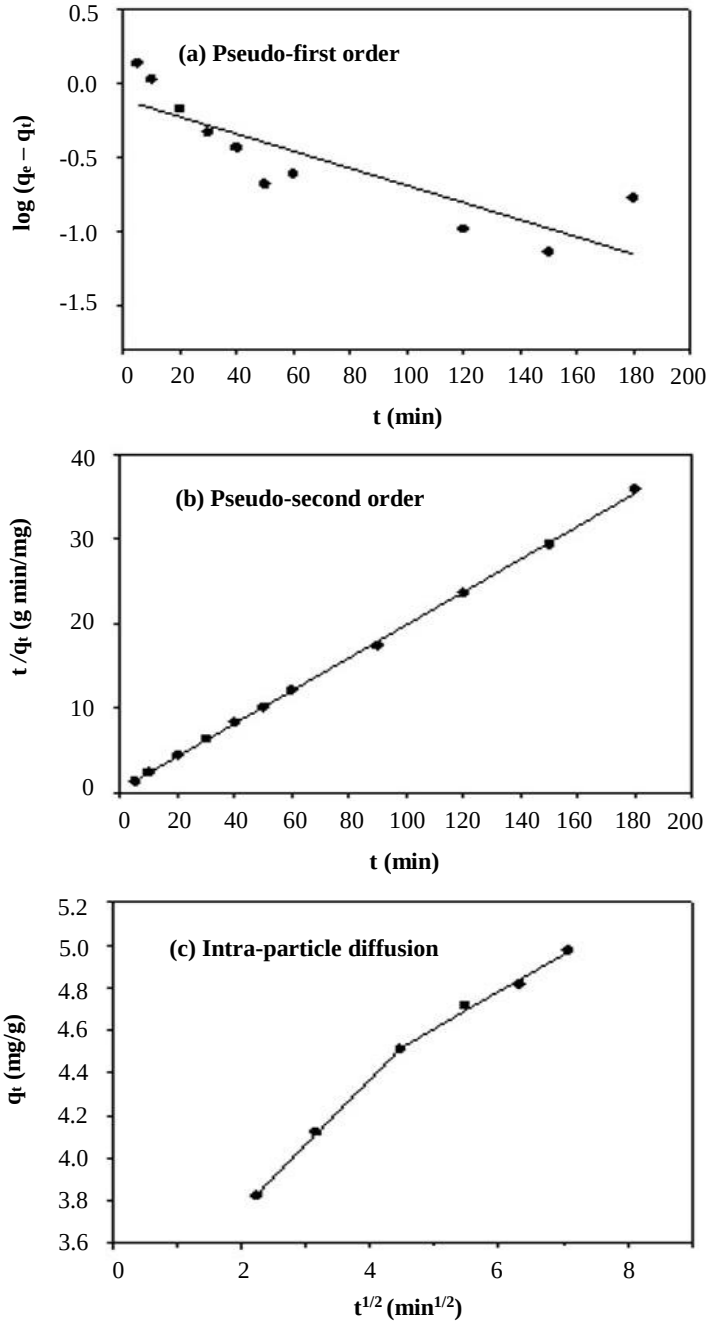

Figure 6 Fitting of the kinetic models for (a) pseudo-first order, (b) pseudo-second order and (c) intra-particle diffusion for adsorption of MB onto optimum carbon.

3.4.2 Adsorption isotherm

The adsorption isotherm is used to determine the interaction between adsorbate and adsorbent and thus to optimize the use of adsorbent [65, 74]. So, the effect of initial dye concentration on the adsorption capacity of the optimum activated carbon was also studied and the results are presented in Figure 7. The amount adsorbed at equilibrium (q_e) increases from ~22 to ~264 mg g^{-1} with an increase in the initial MB concentration from 30 to 600 mg L^{-1}. This indicates that the HDL-derived carbon was very efficient to remove MB cationic dye from aqueous solutions over a large concentration range. The isotherm presents a large increase in the adsorption capacity at low MB concentrations followed by a plateau as the concentration increases.

Table 4 Parameters from kinetic models of the MB adsorption by using optimum carbon.

Model	Value
$q_{e,exp}$ (mg g^{-1})	5.181
Pseudo-first order	
$q_{e,cal}$ (mg g^{-1})	0.771
k_1 (min^{-1})	0.013
R^2	0.729
Pseudo-second order	
$q_{e,cal}$ (mg g^{-1})	5.139
k_2 (g mg^{-1} min^{-1})	0.096
R^2	0.999
Intra-particle diffusion	
Stage 1:	
k_d (mg g^{-1} min$^{-1/2}$)	0.306
C (mg g^{-1})	3.145
R^2	0.999
Stage 2:	
k_d (mg g^{-1} min$^{-1/2}$)	0.172
C (mg g^{-1})	3.748
R^2	0.990

The Langmuir and Freundlich non-linear isotherm models were applied to the MB adsorption isotherm data. The Langmuir isotherm assumes monolayer adsorption and the sorbent contains a finite number of adsorption sites, uniform energy of adsorption and no transmigration of adsorbate in plane of surface [68]. The mathematical expression of this model is given by:

$$q_e = \frac{q_m K_L C_e}{1 + K_L C_e} \tag{11}$$

where q_m (mg g^{-1}) and K_L (L mg^{-1}) are the maximum monolayer adsorption capacity and the Langmuir adsorption equilibrium constant related to the adsorption rate, respectively. The Langmuir dimensionless separation factor (R_L) can be determined by:

$$R_L = \frac{1}{1 + K_L C_o} \tag{12}$$

where C_o is the initial concentration of dye. This factor indicates the possibility of the adsorption process i.e. favorable adsorption when $0 < R_L < 1$, unfavorable adsorption when R_L higher than 1, linear adsorption when R_L equal to 1 and irreversible adsorption when R_L equal to 0 [65].

The Freundlich model is based on heterogeneous surface energies of the adsorbent and assumes that the adsorbate first occupies the strong binding sites until all sites are exhausted [75]. The Freundlich isotherm also assumes multilayer adsorption and the adsorption capacity is related to the adsorbate concentration at equilibrium [76]. The non-linear form of this model is:

$$q_e = K_F C_e^{1/n} \tag{13}$$

where K_F ((mg g^{-1})·(L mg^{-1})$^{1/n}$) and n are the constant associated with the binding energy and the tendency of adsorption, respectively. A value of $1/n$ below 1 indicates a normal Langmuir isotherm, $1/n$ above 1 is indicative of cooperative adsorption [50] while $1/n = 1$ is a linear adsorption isotherm. Moreover a value of n between 1 and 10 indicates favorable adsorption, while $n < 0.5$ is unfavorable [65, 77].

The non-linear fitting curves resulting from both isotherms are presented in Figure 7 and the calculated constants and R^2 are summarized in Table 5. When comparing the two models, the Langmuir model described the experimental data better than the Freundlich model because its R^2 was closer to unity. This suggests that adsorption of MB mainly occurs as a monolayer onto homogeneous sites at the internal and external surfaces of activated carbon. All values of R_L lie between 0 and 1 (Figure 8), indicating that the adsorption process was favorable. Furthermore, the $1/n$ value of 0.450 and the n value of 2.222 obtained from the Freundlich model indicated a normal Langmuir isotherm and the MB adsorption onto HDL-derived activated carbon is favorable. The same observation that MB adsorption onto biomass-based carbon followed the Langmuir isotherm was previously found by Dod et al. [15], Oliveira et al. [38], Lin et al. [65] and Tan et al. [68].

Table 5 Adsorption isotherm parameters for MB adsorption on optimum activated carbon.

Model	Value
Langmuir	
q_m (mg g^{-1})	338.86
K_L (L mg^{-1})	0.012
R^2	0.990
Freundlich	
K_F ((mg g^{-1})·(L mg^{-1})$^{1/n}$)	21.544
$1/n$	0.450
R^2	0.952

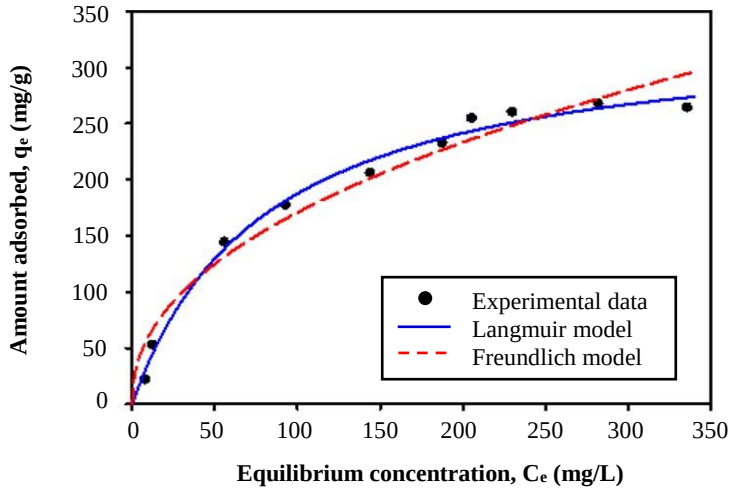

Figure 7 Adsorption isotherm of MB on HDL carbon from experimental and correlated by Langmuir and Freundlich models.

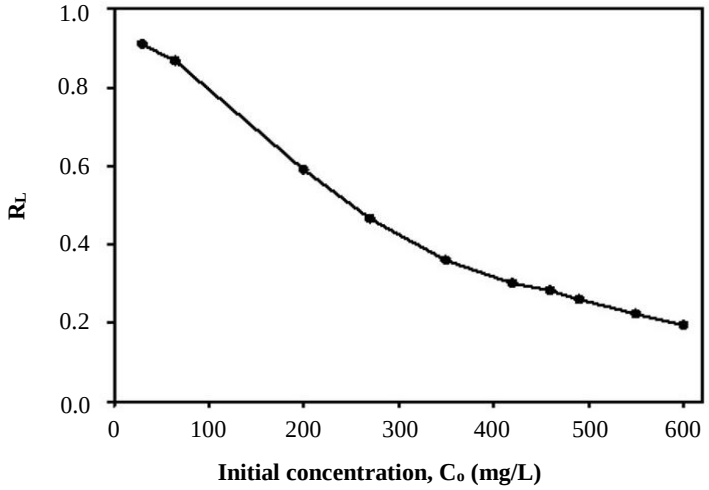

Figure 8 Separation factor (R_L) of Langmuir isotherm.

The maximum adsorption capacity of MB (q_m) onto the HDL-derived carbon was 338.86 mg g^{-1}, which is comparable to or higher than activated carbons from various other biomasses (Table 6). Therefore, the prepared carbon could be used as an effective adsorbent for this purpose. Moreover, it can be seen that the amount of MB adsorbed not only depended on the surface area of the activated carbon, because some materials with a higher surface area had a lower adsorption capacity. Therefore, the adsorption of MB by activated carbon was also dependent on surface chemistry (surface functional groups and surface charge). In addition, the suitable activated carbon for removal of MB from solution should contain plenty mesopores due to the larger molecular size of dye compared to gas molecules.

Table 6 Comparison of maximum adsorption capacity for MB by HDL-derived carbon with other biomass-based carbons.

Raw material	Activating agent	Surface area (m^2 g^{-1})	Mesoporosity (%)	Adsorption capacity (mg g^{-1})
Hydrolyzed *Dipterocarpus alatus* leaves (HDL)	$ZnCl_2$	497	21	338.86
Hazelnut husk [72]	H_3PO_4	770	-	204.00
Cotton stalks [22]	KOH	950	29	222.00
Jute fiber [24]	H_3PO_4	-	-	225.64
Watermelon rind [17]	$ZnCl_2$	1,156	94	231.48
Oil palm shell [25]	KOH	596	-	243.90
Date stone [26]	$FeCl_3$	780	22	259.25
Buriti shell [5]	$ZnCl_2$	843	25	274.62
Piassava fibers [27]	$ZnCl_2$	1,190	2	276.40
Oil palm fibre [68]	KOH	1,354	-	277.78
Jackfruit peel [28]	H_3PO_4	1,261	36	280.30
Pineapple leaves [41]	$ZnCl_2$	914	73	288.34
Fruit of *Catalpa bignonioides* [14]	$ZnCl_2$	896	93	299.40
Walnut shell [29]	$ZnCl_2$	1,800	-	315.00
Black stone cherries [30]	H_3PO_4	-	-	321.75
Waste cotton fiber [31]	H_3PO_4	694	19	344.82
Date stone [7]	$ZnCl_2$	1,046	-	398.19

4. Conclusions

In this work, activated carbons were prepared via pyrolysis of hydrolyzed *Dipterocarpus alatus* leaves (HDL) treated with $ZnCl_2$ as activating agent. The effect of treatment time on the porous characteristics of carbons was examined, and the maximum surface area was 497 m^2 g^{-1} for a treatment time of 12 h. This optimum carbon was also characterized by TG, FTIR, proximate analysis, bulk density and pH. The optimum activated carbon was a very efficient adsorbent for the color removal of methylene blue (MB) from aqueous solution. Kinetic data followed a pseudo-second order model indicating a chemisorption process. The intra-particle diffusion model suggests that adsorption of MB onto activated carbon was controlled by both film as well as pore diffusion mechanism. The adsorption behavior is well described by Langmuir isotherm (R^2 = 0.990). The maximum monolayer adsorption capacity of 338.86 mg g^{-1} is comparable to or higher than several biomass-based activated carbons reported in the literature. As a conclusion, hydrolyzed *Dipterocarpus alatus* leaves, a solid waste residue from production of biodiesel, can be utilized as a low-cost material for the production of activated carbon and is a promising sustainable adsorbent for the color removal of dyes from wastewater.

5. Acknowledgements

The authors would like to thank the financial support from the National Research Council of Thailand (Grant No. 41/2563) for funding this research.

6. Disclosure statement

There are no conflicts of interest to declare.

7. References

[1] Kumar D, Singh B, Korstad J. Utilization of lignocellulosic biomass by oleaginous yeast and bacteria for production of biodiesel and renewable diesel. Renew Sustain Energy Rev. 2017;73:654-71.
[2] Wi SG, Cho EJ, Lee DS, Lee SJ, Lee YJ, Bae HJ. Lignocellulose conversion for biofuel: a new pretreatment greatly improves downstream biocatalytic hydrolysis of various lignocellulosic materials. Biotechnol Biofuels. 2015;8:228:1-11.
[3] Kamyo T, Asanok L. Modeling habitat suitability of *Dipterocarpus alatus* (Dipterocarpaceae) using MaxEnt along the Chao Phraya River in Central Thailand. For Sci Technol. 2020;16(1):1-7.
[4] Heidari A, Younesi H, Rashidi A, Ghoreyshi A. Adsorptive removal of CO_2 on highly microporous activated carbons prepared from *Eucalyptus camaldulensis* wood: effect of chemical activation. J Taiwan Inst Chem Eng. 2014;45(2):579-88.
[5] Pezoti O, Cazetta AL, Souza IPAF, Bedin KC, Martins AC, Silva TL, et al. Adsorption studies of methylene blue onto $ZnCl_2$-activated carbon produced from buriti shells (*Mauritia flexuosa* L.). J Ind Eng Chem. 2014;20(6):4401-7.
[6] Reffas A, Bernardet V, David B, Reinert L, Lehocine MB, Dubois M, et al. Carbons prepared from coffee grounds by H_3PO_4 activation: characterization and adsorption of methylene blue and Nylosan Red N-2RBL. J Hazard Mater. 2010;175(1-3):779-88.
[7] Ahmed MJ, Dhedan SK. Equilibrium isotherms and kinetics modeling of methylene blue adsorption on agricultural waste-based activated carbons. Fluid Ph Equilibria. 2012;317:9-14
[8] Rashid RA, Jawad AH, Mohd Azlan MI, Kasim NN. $FeCl_3$-activated carbon developed from coconut leaves: characterization and application for methylene blue removal. Sains Malays. 2018;47(3):603-10.
[9] Anisuzzaman SM, Joseph CG, Daud WMABW, Krishnaiah D, Yee HS. Preparation and characterization of activated carbon from *Typha orientalis* leaves. Int J Ind Chem. 2015;6:9-21.
[10] Martín-González MA, Susial P, Pérez-Pena J, Dona-Rodríquez JM. Preparation of activated carbons from banana leaves by chemical activation with phosphoric acid: adsorption of methylene blue. Rev Mex Ing Quím. 2013;12(3):595-608.
[11] Patil D, Chavan S, Barkade S. Production of activated charcoal from sugar cane leaves using $ZnCl_2$ activation for the adsorption of methylene blue dye. Int J Eng Res Technol. 2013;2(3):1-5.
[12] Elhussien MH, Hussein RM, Nimir SA, Elsaim MH. Preparation and characterization of activated carbon from palm tree leaves impregnated with zinc chloride for the removal off lead (II) from aqueous solutions. Am J Phys Chem. 2017;6(4):59-69.
[13] Xu J, Chen L, Qu H, Jiao Y, Xie J, Xing G. Preparation and characterization of activated carbon from reedy grass leaves by chemical activation with H_3PO_4. Appl Surf Sci. 2014;320:674-80.
[14] Geçgel Ü, Kocabıyık B, Üner O. Adsorptive removal of methylene blue from aqueous solution by the activated carbon obtained from the fruit of *Catalpa bignonioides*. Water Air Soil Pollut. 2015;226(8):238.
[15] Dod R, Banerjee G, Saini DR. Removal of methylene blue (MB) dye from water environment by processed Jowar Stalk [*Sorghum bicolor* (L.) Moench] adsorbent. Clean Technol Environ Policy. 2015;17:2349-59.
[16] Mahmoodi NM. Photodegradation of dyes using multiwalled carbon nanotube and ferrous ion. J Environ Eng. 2013;139(11):1368-74.
[17] Üner O, Geçel Ü, Bayrak Y. Adsorption of methylene blue by an efficient activated carbon prepared from *Citrullus lanatus* Rind: kinetics, isotherm, thermodynamic, and mechanism analysis. Water Air Soil Pollut. 2016;227:247.
[18] Mahmoodi NM, Oveisi M, Taghizadeh A, Taghizadeh M. Novel magnetic amine functionalized carbon nanotube/metal-organic framework nanocomposites: from green ultrasound-assisted synthesis to detailed selective pollutant removal modelling from binary systems. J Hazard Mater. 2019;368:746-59.
[19] Mahmoodi NM, Taghizadeh M, Taghizadeh A, Abdi J, Hayati B, Shekarchi AA. Bio-based magnetic metal-organic framework nanocomposite: ultrasound-assisted synthesis and pollutant (heavy metal and dye) removal from aqueous media. Appl Surf Sci. 2019;480:288-99.
[20] Mahmoodi NM, Abdi J, Bastani D. Direct dyes removal using modified magnetic ferrite nanoparticle. J Environ Health Sci Eng. 2014;12:96.
[21] Attia AA, Girgis BS, Fathy NA. Removal of methylene blue by carbons derived from peach stones by H_3PO_4 activation: batch and column studies. Dyes Pigm. 2008;76(1):282-9.

[22] Fathy NA, Girgis BS, Khalil LB, Farah JY. Utilization of cotton stalks-biomass waste in the production of carbon adsorbents by KOH activation for removal of dye-contaminated water. Carbon Lett. 2010;11(3):224-34.
[23] Girgis BS, Soliman AM, Fathy NA. Development of micro-mesoporous carbons from several seed hulls under varying conditions of activation. Microporous Mesoporous Mater. 2011;142(2-3):518-25.
[24] Senthilkumaar S, Varadarajan PR, Porkodi K, Subbhuraam CV. Adsorption of methylene blue onto jute fiber carbon: kinetics and equilibrium studies. J Colloid Interface Sci. 2005;284(1):78-82.
[25] Tan IAW, Ahmad AL, Hameed BH. Adsorption of basic dye using activated carbon prepared from oil palm shell: batch and fixed bed studies. Desalination. 2008;225(1-3):13-28.
[26] Theydan SK, Ahmed MJ. Adsorption of methylene blue onto biomass-based activated carbon by $FeCl_3$ activation: equilibrium, kinetics, and thermodynamic studies. J Anal Appl Pyrolysis. 2012;97:116-22.
[27] Avelar FF, Bianchi ML, Gonçalves M, da Mota EG. The use of piassava fibers (*Attalea funifera*) in the preparation of activated carbon. Bioresour Technol. 2010;101(12):4639-45.
[28] Prahas D, Kartika Y, Indraswati N, Ismadji S. The use of activated carbon prepared from jackfruit (*Artocarpus heterophyllus*) peel waste for methylene blue removal. J Environ Prot Sci. 2008;2:1-10.
[29] Yang J, Qiu K. Preparation of activated carbons from walnut shells via vacuum chemical activation and their application for methylene blue removal. Chem Eng J. 2010;165(1):209-17.
[30] Arana JMRR, Mazzoco RR. Adsorption studies of methylene blue and phenol onto black stone cherries prepared by chemical activation. J Hazard Mater. 2010;180(1-3):656-61.
[31] Ekrami E, Dadashian F, Arami M. Adsorption of methylene blue by waste cotton activated carbon: equilibrium, kinetics, and thermodynamic studies. Desalination Water Treat. 2016;57(15):7098-108.
[32] Khangwichian W, Pattamasewe S, Laungphairojana A, Leesing R, Hunt AJ, Ngernyen Y. Preparation of activated carbons from hydrolyzed *Dipterocarpus alatus* leaves: value added product from biodiesel production waste. J Jpn Inst Energy. 2021;100(10):219-24.
[33] Ahmedna M, Johns MM, Clarke SJ, Marshall WE, Rao RM. Potential of agricultural by-product-based activated carbons for use in raw sugar decolourisation. J Sci Food Agric. 1997;75(1):117-24.
[34] Ekpete OA, Marcus AC, Osi V. Preparation and characterization of activated carbon obtained from Plantain (*Musa paradisiaca*) fruit stem. J Chem. 2017;2017:8635615.
[35] Yorgun S, Yıldzı D. Preparation and characterization of activated carbons from Paulownia wood by chemical activation with H_3PO_4. J Taiwan Inst Chem Eng. 2015;53:122-31.
[36] Sharath D, Ezana J, Shamil Z. Production of activated carbon from solid waste rice peel (husk) using chemical activation. J Ind Pollut Control. 2017;33(2):1132-9.
[37] Ravichandran P, Sugumaran P, Seshadri S, Basta AH. Optimizing the route for production of activated carbon from *Casuarina equisetifolia* fruit waste. R Soc Open Sci. 2018;5(7):171578.
[38] de Oliveira GF, de Andrade RC, Trindade MAG, Andrade HMC, de Carvalho CT. Thermogravimetric and spectroscopic study (TG-DTA/FT-IR) of activated carbon from the renewable biomass source Babassu. Quim Nova. 2017;40(3):284-92.
[39] Wu L, Shang Z, Wang H, Wan W, Gao X, Li Z, et al. Production of activated carbon from walnut shell by CO_2 activation in a fluidized bed reactor and its adsorption performance of copper ion. J Mater Cycles Waste Manag. 2018;20:1676-88.
[40] Angın D, Altintig E, Köse TE. Influence of process parameters on the surface and chemical properties of activated carbon obtained from biochar by chemical activation. Bioresour Technol. 2013;148:542-9.
[41] Mahamad MN, Zaini MAA, Zakaria ZA. Preparation and characterization of activated carbon from pineapple waste biomass for dye removal. Int Biodeterior Biodegradation. 2015;102:274-80.
[42] Yagmur E, Gokce Y, Tekin S, Semerci NI, Aktas Z. Characteristics and comparison of activated carbons prepared from oleaster (*Elaeagnus angustifolia* L.) fruit using KOH and $ZnCl_2$. Fuel. 2020;267:117232.
[43] Budi E, Nasbey H, Yuniarti BDP, Nurmayatri Y, Fahdiana J, Budiet AS. Pore structure of the activated coconut shell charcoal carbon. AIP Conf Proc. 2014;1617(1):130-3.
[44] Gupta A, Garg A. Primary sewage sludge-derived activated carbon: characterisation and application in wastewater treatment. Clean Technol Environ Policy. 2015;17(6):1619-31.
[45] Xie B, Qin J, Wang S, Li X, Sun H, Chen W. Adsorption of phenol on commercial activated carbons: modelling and interpretation. Int J Environ Res Public Health. 2020;17(3):789.
[46] de Souza Macedo J, da Costa Júnior NB, Almeida LE, da Silva Vieira EF, Cestari AR, Gimenez IF, et al. Kinetic and calorimetric study of the adsorption of dyes on mesoporous activated carbon prepared from coconut coir dust. J Colloid Interface Sci. 2006;298(2):515-22.
[47] Abdullah AH, Kassim A, Zainal Z, Hussien MZ, Kuang D, Ahmad F, et al. Preparation and characterization of activated carbon from gelam wood bark (*Melaleuca cajuputi*). Malaysian J Anal Sci. 2001;7(1):65-8.
[48] Asadullah M, Rahman MA, Motin MA, Sultan MB. Preparation and adsorption studies of high specific surface area activated carbons obtained from the chemical activation of jute stick. Adsorp Sci Technol. 2006;24(9):761-70.
[49] Pastor-Villegas J, Pastor-Valle JF, Meneses Rodríguez JM, García García M. Study of commercial wood charcoals for the preparation of carbon adsorbents. J Anal Appl Pyrolysis. 2006;76(1-2):103-8.
[50] Rozada F, Otero M, Morán A, García AI. Activated carbons from sewage sludge and discarded tyres: production and optimization. J Hazard Mater. 2005;124(1-3):181-91.
[51] AL-Othman ZA, Ali R, Naushad Mu. Hexavalent chromium removal from aqueous medium by activated carbon prepared from peanut shell: adsorption kinetics, equilibrium and thermodynamic studies. Chem Eng J. 2012;184:238-47.
[52] Abech SE, Gimba CE, Uzairu A, Dallatu YA. Preparation and characterization of activated carbon from palm kernel shell by chemical activation. Res J Chem Sci. 2013;3(7):54-61.
[53] Shamsuddin MS, Yusoff NRN, Sulaiman MA. Synthesis and characterization of activated carbon produced from Kenaf core fiber using H_3PO_4 activation. Procedia Chem. 2016;19:558-65.
[54] Valliammai S, Subbareddy Y, Nagaraja KS, Jeyaraj B. Removal of methylene blue from aqueous solution by activated carbon of *Vigna mungo L* and *Paspalum scrobiculatum*: equilibrium, kinetics and thermodynamic studies. Indian J Chem Technol. 2017;24:134-44.

[55] Dao TM, Le Luu T. Synthesis of activated carbon from macadamia nutshells activated by H_2SO_4 and K_2CO_3 for methylene blue removal in water. Bioresour Technol Rep. 2020;12:100583.
[56] Uçar S, Erdem M, Tay T, Karagöz S. Preparation and characterization of activated carbon produced from pomegranate seeds by $ZnCl_2$ activation. Appl Surf Sci. 2009;255(21):8890-6.
[57] Amerkhanova S, Shlyapov R, Uali A. The active carbons modified by industrial wastes in process of sorption concentration of toxic organic compounds and heavy metals ions. Colloids Surf A Physicochem Eng Asp. 2017;532:36-40.
[58] Bazan A, Nowicki P, Półrolniczak P, Pietrzak R. Thermal analysis of activated carbon obtained from residue after supercritical extraction of hops. J Therm Anal Calorim. 2016;125(3):1199-204.
[59] Álvarez-Torrellas S, Ovejero G, García-Lovera R, Rodríquez A, García J. Synthesis of a mesoporous carbon from peach stones for adsorption of basic dyes from wastewater: kinetics, modeling, and thermodynamic studies. Clean Technol Environ Policy. 2016;18(4):1085-96.
[60] Ilomuanya MO, Nashiru B, Ifudu ND, Igwilo CI. Effect of pore size and morphology of activated charcoal prepared from midribs of *Elaeis guineensis* on adsorption of poisons using metronidazole and *Escherichia coli* O157:H7 as a case study. J Microsc Ultrastruct. 2017;5(1):32-8.
[61] Hidayu AR, Mohamad NF, Matali S, Sharifah ASAK. Characterization of activated carbon prepared from oil palm empty fruit bunch using BET and FT-IR techniques. Procedia Eng. 2013;68:379-84.
[62] Ademiluyi FT, David-West EO. Effect of chemical activation on the adsorption of heavy metals using activated carbons from waste materials. ISRN Chem Eng. 2012;2012:674209.
[63] Ahmad AL, Loh MM, Aziz JA. Preparation and characterization of activated carbon from oil palm wood and its evaluation on methylene blue adsorption. Dyes Pigm. 2007;75(2):263-72.
[64] Verma P, Samanta SK. A direct method to determine the adsorbed dyes on adsorbent via processing of diffuse reflectance spectroscopy data. Mater Res Express. 2018;6(1):015505.
[65] Lin L, Zhai SR, Xiao ZY, Song Y, An QD, Song XW. Dye adsorption of mesoporous activated carbons prepared from NaOH-pretreated rice husks. Bioresour Technol. 2013;136:437-43.
[66] Marrakchi F, Ahmed MJ, Khanday WA, Asif M, Hameed BH. Mesoporous-activated carbon prepared from chitosan flakes via single-step sodium hydroxide activation for the adsorption of methylene blue. Int J Biol Macromol. 2017;98:233-9.
[67] Pathania D, Sharma S, Singh P. Removal of methylene blue by adsorption onto activated carbon developed from *Ficus carica* bast. Arab J Chem. 2017;10:1445-51.
[68] Tan IAW, Hameed BH, Ahmad AL. Equilibrium and kinetic studies on basic dye adsorption by oil palm fibre activated carbon. Chem Eng J. 2007;127(1-3):111-9.
[69] Sogbochi E. Evaluation of adsorption capacity of methylene blue in aqueous medium by two adsorbents: the raw hull of *Lophira Lanceolata* and its activated carbon. Am J Phys Chem. 2017;6(5):76-87.
[70] Hameed BH, Din AT, Ahmad AL. Adsorption of methylene blue onto bamboo-based activated carbon: kinetics and equilibrium studies. J Hazard Mater. 2007;141(3):819-25.
[71] Ahmad F, Daud WMAW, Ahmad MA, Radzi R. Cocoa (*Theobroma cacao*) shell-based activated carbon by CO_2 activation in removing of cationic dye from aqueous solution: kinetics and equilibrium studies. Chem Eng Res Des. 2012;90(10):1480-90.
[72] Ozer C, Imamoglu M, Turhan Y, Boysan F. Removal of methylene blue from aqueous solutions using phosphoric acid activated carbon produced from hazelnut husks. Toxicol Environ Chem. 2012;94(7):1283-93.
[73] Bağci S, Ceyhan AA. Adsorption of methylene blue onto activated carbon prepared from *Lupinus albus*. Chem Ind Chem Eng Q. 2016;22(2):155-65.
[74] Aygün A, Yenisoy-Karakaş S, Duman I. Production of granular activated carbon from fruit stones and nutshells and evaluation of their physical, chemical and adsorption properties. Microporous Mesoporous Mater. 2003;66(2-3):189-95.
[75] Yu X, Han Z, Fang S, Chang C, Han X. Optimized preparation of high value-added activated carbon and its adsorption properties for methylene blue. Int J Chem React Eng. 2019;17(8):20180267.
[76] Rai P, Gautam RK, Banerjee S, Rawat V, Chattoapadhyaya MC. Synthesis and characterization of a novel $SnFe_2O_4$@activated carbob magnetic nanocomposite and its effectiveness in the removal of crystal violet from aqueous solution. J Environ Chem Eng. 2015;3(4):2281-91.
[77] Puttamat S, Pavarajarn V. Adsorption study for removal of Mn (II) ion in aqueous solution by hydrated ferric (III) oxides. Int J Chem Eng Appl. 2016;7(4):239-43.